Steel and Composite Structures, *Vol. 35, No. 4* (*2020*) *545-554*
DOI: https://doi.org/10.12989/scs.2020.35.4.545

Nonlocal nonlinear dynamic behavior of composite piezo-magnetic beams using a refined higher-order beam theory

Raad M. Fenjan, Ridha A. Ahmed and Nadhim M. Faleh*

Al-Mustansiriah University, Engineering Collage P.O. Box 46049, Bab-Muadum, Baghdad 10001, Iraq

(*Received January 16, 2020, Revised April 20, 2020, Accepted April 23, 2020*)

Abstract. The present paper explores nonlinear dynamical properties of piezo-magnetic beams based on a nonlocal refined higher-order beam formulation and piezoelectric phase effect. The piezoelectric phase increment may lead to improved vibrational behaviors for the smart beams subjected to magnetic fields and external harmonic excitation. Nonlinear governing equations of a nonlocal intelligent beam have been achieved based upon the refined beam model and a numerical provided has been introduced to calculate nonlinear vibrational curves. The present study indicates that variation in the volume fraction of piezoelectric ingredient has a substantial impact on vibrational behaviors of intelligent nanobeam under electrical and magnetic fields. Also, it can be seen that nonlinear free/forced vibrational behaviors of intelligent nanobeam have dependency on the magnitudes of induced electrical voltages, magnetic potential, stiffening elastic substrate and shear deformation.

Keywords: refined beam**;** dynamic behavior**;** forced vibration; free vibration; piezoelectric reinforcement; nonlocal theory

1. Introduction

Recently, the development in the field of engineering materials has disclosed the advantages associated with the smart/intelligent materials (Sahu *et al*. 2018, Singhal *et al*. 2018). Incorporation of these smart materials in various multifunctional structures has paved way for tremendous changes in different engineering fields. Among them, magneto-electro-elastic (MEE) materials are unique as a matter of fact that it exhibits triple energy conversion between elastic, electrical and magnetic fields (Pan and Han 2005, Li and Hu 2016). Therefore, it has become a potential candidate for sophisticated applications such as vibration control, energy harvesting, sensors and actuators etc. More recently, attempts were made to synthesize MEE structures through composite materials and improvise the structural functionalities. For example, the mechanical characteristics of multi-phase MEE materials may be controlled via the variation of material composition and portion of each phase (Mirjavadi *et al*. 2019, Ahmed *et al.* 2019). Having realized that the smart structures made of magneto-electro-elastic materials with different material composition play a significant role in industrial fields many pioneers have devoted their research to assess the mechanical response in various working environments (Kumaravel *et al.* 2007, Annigeri *et al.* 2007).

At nano range, significant influence of size effects is noticed on both physical as well as the mechanical properties. This phenomenon has motivated few researchers to divert their focus towards assessing the mechanical response of the nanostructures. The major limitation of the classical continuum mechanics is its inefficiency to model small size structures which paved way for the establishment of higher order continuum theories which incorporates the size dependency of structure with ease (Boutaleb *et al.* 2019, Tlidji *et al*. 2019, Semmah *et al.* 2019, She *et al*. 2018, Saffari *et al*. 2017, Soltani *et al*. 2019). The Eringen's nonlocal elasticity theory (Eringen 1972) proved to be handy in employing the size-effects. Due to the reason that performing experiment on a nano-size structure is still hard, many articles have been published to make the best utilization of this theory in evaluating the size-dependent structural response (Li *et al.* 2018, Al-Maliki *et al.* 2019, Uzun and Civalek 2019, Wu *et al.* 2018). The major outcome of these researches indicate that with the higher value of nonlocal parameter, that nonlocal elastic models are efficient enough only to yield stiffness-softening effect. Incorporating the Eringen's nonlocal elasticity theory few researchers attempted to analyze the MEE or piezo-magnetic nanostructures. With usage of nonlocal theory, a study on linear vibrational properties of intelligent nano-size beams has been represented by Ke and Wang (2014). Moreover, Jandaghian and Rahmani (2016) represented linear vibrational investigation of intelligent nano-size beams based on elastic foundations. In another research, vibrational properties of a functionally graded intelligent nano-scale beam with usage of nonlocal theory have been examined by Ebrahimi and Barati (2017).

In view of the above, the aim of the present article is to develop a multi-phase MEE nanobeam resting on nonlinear elastic substrate for dynamical analysis within the framework of nonlocal elasticity theory. It is supposed that the MEE composite has two phases with piezoelectric and magnetic constituents. Eringen's elasticity theory is served

*Corresponding author, Professor
E-mail: dr.nadhim@uomustansiriyah.edu.iq

ISSN: 1229-9367 (Print), 1598-6233 (Online)

Table 1 Material constants for $BaTiO_3$-$CoFe_2O_4$ composite

Property	V_f=0	V_f=0.2	V_f=0.4	V_f=0.6	V_f=0.8
C_{11} *(GPa)*	286	250	225	200	175
C_{13}	170	145	125	110	100
C_{33}	269.5	240	220	190	170
e_{31} *(C/m^2)*	0	-2	-3	-3.5	-4
e_{33}	0	4	7	11	14
q_{31} *(N/Am)*	580	410	300	200	100
q_{33}	700	550	380	260	120
k_{11} *(10^{-9} C/Vm)*	0.08	0.33	0.8	0.9	1
k_{33}	0.093	2.5	5	7.5	10
d_{11} *(10^{-12} Ns/VC)*	0	2.8	4.8	6	6.8
d_{33}	0	2000	2750	2500	1500
x_{11} *(10^{-4} Ns^2/C^2)*	-5.9	-3.9	-2.5	-1.5	-0.8
x_{33}	1.57	1.33	1	0.75	0.5
ρ *(kg/m^3)*	5300	5400	5500	5600	5700

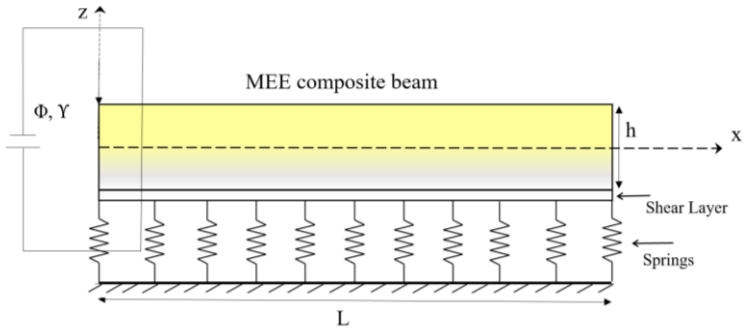

Fig. 1 A piezo-magnetic composite nanobeam rested on elastic substrate

to study the nano-scale effect. Additionally, the equilibrium equations of nanobeam with MEE properties are derived utilizing Hamilton's principle and von-Kármán geometric nonlinearity. Then, an approximate solution based on Galerkin's technique has been provided. A parametrical study is carried out to examine the influence of nonlocality, various piezoelectric volume, electro-magnetic field and elastic substrate coefficients on the structural performance of such nano-scale systems. The results of this paper can be a good reference for designing and optimizing the smart structures under dynamic loads.

2. Two-phase composite of magneto-electro-elastic type

Fig. 1 indicates a nano-scale beam made of magneto-electro-elastic composite with two phases. Material properties of multi-phase MEE composite rely on the percentage and volume of piezoelectric phase (V_f). This article studies a nanobeam constructed by a composite of $BaTiO_3$-$CoFe_2O_4$ for which Table 1 is devoted to represent the material properties. For such materials, $BaTiO_3$ denotes the piezo-electrical ingredient and also $CoFe_2O_4$ denotes the piezo-magnetic ingredient. Based on Table 1, elastic (C_{ij}), piezo-electrical (e_{ij}) and magneto-electric (q_{ij}) parameters have been presented. Furthermore, k_{ij}, d_{ij} and x_{ij} indicate the dielectric, magneto-electrical and magnetic permeability coefficients, respectively.

3. Formulation according to refined beam theory

So far, different beam and plate theories are available in the literature (Fenjan *et al*. 2019, Zarga *et al.* 2019, Chaabane *et al.* 2019, Mahmoudi *et al*. 2019, Medani *et al*. 2019, Besseghier *et al*. 2015, Abdelaziz *et al*. 2017, Atmane *et al*. 2015, Bounouara *et al.* 2016, Bellifa *et al*. 2017, Boukhlif *et al.* 2019). In this section, the procedure of obtaining governing equations for a piezo-magnetic nanobeam will be presented in the context of nonlocal and classic beam theories. For achieving this goal, the

displacement field of nano-scale beam based on axial (u) and transverse (w) displacements at the mid-axis may be written as (Fourn *et al*. 2018)

$$u_1(x,z,t)=u(x,t)-z\frac{\partial w_b}{\partial x}-\square(z)\frac{\partial w_s}{\partial x} \tag{1}$$

$$u_3(x,z,t)=w(x,t)=w_b(x)+w_s(x) \tag{2}$$

where $\square(z)=z-\sin(\beta z)/\beta$. For considering geometric nonlinearity, the axial strain of the beam should be written as

$$\begin{aligned}\varepsilon_{xx}&=\frac{\partial u_1}{\partial x}=\frac{\partial u}{\partial x}-z\frac{\partial^2 w_b}{\partial x^2}+\frac{1}{2}(\frac{\partial w}{\partial x})^2-h(z)\frac{\partial^2 w_s}{\partial x^2}\\ \gamma_{xz}&=r(z)\frac{\partial w_s}{\partial x}\end{aligned} \tag{3}$$

In this research, it is supposed that electric voltage (V_E) and magnetic field intensity (Ω) due to magnetic $\Upsilon(x,z,t)$ and electrical $\Phi(x,z,t)$ field potentials are applied to the nano-size beam. The potentials can be expressed in the form

$$\Phi(x,y,z,t)=-\cos(\beta z)\phi(x,y,t)+\frac{2z}{h}V_E \tag{4}$$

$$\Upsilon(x,y,z,t)=-\cos(\beta z)\gamma(x,y,t)+\frac{2z}{h}\Omega \tag{5}$$

where $\beta=\pi/h$. Above potentials lead to induction of electrical field (E_x,E_z) and magnetic field (H_x,H_z) in x and z directions which can be derived via Eqs. (4) and (5) as

$$E_x=-\Phi_{,x}=\cos(\beta z)\frac{\partial\phi}{\partial x},\quad E_z=-\Phi_{,z}=-\beta\sin(\beta z)\phi-\frac{2V_E}{h} \tag{6}$$

$$H_x=-\Upsilon_{,x}=\cos(\beta z)\frac{\partial\gamma}{\partial x},\quad H_z=-\Upsilon_{,z}=-\beta\sin(\beta z)\gamma-\frac{2\Omega}{h} \tag{7}$$

There are five coupled governing equations for a refined multi-phase piezo-magnetic nano-size beam embedded on elastic substrate which can be derived via Hamilton's principle as

$$\frac{\partial N_x}{\partial x}=I_0\frac{\partial^2 u}{\partial t^2}-I_1\frac{\partial^3 w_b}{\partial x\partial t^2}-J_1\frac{\partial^3 w_s}{\partial x\partial t^2} \tag{8}$$

$$\begin{aligned}&\frac{\partial^2 M_x^b}{\partial x^2}+\frac{\partial}{\partial x}(N_x[\frac{\partial w}{\partial x}])-k_L(w_b+w_s)+k_P\frac{\partial^2(w_b+w_s)}{\partial x^2}-k_{NL}w^3\\ &=f(t)+I_0\frac{\partial^2(w_b+w_s)}{\partial t^2}+I_1(\frac{\partial^3 u}{\partial x\partial t^2})-I_2\nabla^2(\frac{\partial^2 w_b}{\partial t^2})-J_2\nabla^2(\frac{\partial^2 w_s}{\partial t^2})\end{aligned} \tag{9}$$

$$\begin{aligned}&\frac{\partial^2 M_x^s}{\partial x^2}+\frac{\partial Q_{xz}}{\partial x}+\frac{\partial}{\partial x}(N_x[\frac{\partial w}{\partial x}])-k_L(w_b+w_s)+k_P\frac{\partial^2(w_b+w_s)}{\partial x^2}-k_{NL}w^3\\ &=f(t)+I_0\frac{\partial^2(w_b+w_s)}{\partial t^2}+J_1(\frac{\partial^3 u}{\partial x\partial t^2})-J_2\nabla^2(\frac{\partial^2 w_b}{\partial t^2})-K_2\nabla^2(\frac{\partial^2 w_s}{\partial t^2})\end{aligned} \tag{10}$$

$$\int_{-h/2}^{h/2}\left(\cos(\beta z)\frac{\partial D_x}{\partial x}+\beta\sin(\beta z)D_z\right)dz=0 \tag{11}$$

$$\int_{-h/2}^{h/2}\left(\cos(\beta z)\frac{\partial B_x}{\partial x}+\beta\sin(\beta z)B_z\right)dz=0 \tag{12}$$

where f(t) is applied harmonic excitation. Also, D_i and B_i display the displacement components of electrical and magnetic fields; k_L, k_P, k_{NL} display linear, shear and non-linear coefficients of elastic layer.

Furthermore, N_x and M_x are corresponding to in-plane forces and bending moments which can be defined by (Barati 2017)

$$\begin{aligned}&(N_x,M_x^b,M_x^s)=\int_A(1,z,\square(z))\sigma_{xx}\,dA,\\ &Q_{xz}=\int_A r(z)\sigma_{xz}\,dA\end{aligned} \tag{13a}$$

and also

$$(I_0,I_1,J_1,I_2,J_2,K_2)=\int_{-h/2}^{h/2}(1,z,\square,z^2,z\square,\square^2)\rho dz \tag{13b}$$

Knowing the fact that considered material is isotropic, one can reach to I_1=0. Next, derived boundary conditions may be denoted by

$$N_x=0 \quad \text{or } u=0 \tag{14}$$

$$\frac{\partial M_x^b}{\partial x}+N_x[\frac{\partial w}{\partial x}]=0 \quad \text{or } w_b=0 \tag{15}$$

$$\frac{\partial M_x^s}{\partial x}+Q_{xz}+N_x[\frac{\partial w}{\partial x}]=0 \quad \text{or } w_s=0 \tag{16}$$

$$\int_{-h/2}^{h/2}\cos(\beta z)D_x\,dz=0 \quad \text{or} \quad \phi=0 \tag{17}$$

$$\int_{-h/2}^{h/2}\cos(\beta z)B_x\,dz=0 \quad \text{or} \quad \gamma=0 \tag{18}$$

Introducing nonlocal parameter ea^2, the constitutive relations for a nano-size piezo-magnetic beam should be written in the following forms (Ke and Wang 2014)

$$(1-(ea)^2\nabla^2)\sigma_{xx}=\tilde{c}_{11}\varepsilon_{xx}-\tilde{e}_{31}E_z-\tilde{q}_{31}H_z \tag{19}$$

$$(1-(ea)^2\nabla^2)\sigma_{xz}=\tilde{c}_{66}\gamma_{xz}-\tilde{e}_{15}E_x-\tilde{q}_{15}H_x \tag{20}$$

$$(1-(ea)^2\nabla^2)D_x=\tilde{e}_{15}\gamma_{xz}+\tilde{k}_{11}E_x+\tilde{d}_{11}H_x \tag{21}$$

$$(1-(ea)^2\nabla^2)D_z=\tilde{e}_{31}\varepsilon_{xx}+\tilde{k}_{33}E_z+\tilde{d}_{33}H_z \tag{22}$$

$$(1-(ea)^2\nabla^2)B_x=\tilde{q}_{15}\gamma_{xz}+\tilde{d}_{11}E_x+\tilde{\chi}_{11}H_x \tag{23}$$

$$(1-(ea)^2\nabla^2)B_z=\tilde{q}_{31}\varepsilon_{xx}+\tilde{d}_{33}E_z+\tilde{\chi}_{33}H_z \tag{24}$$

where $\tilde{c}_{ij},\tilde{e}_{ij},\tilde{q}_{ij},\tilde{d}_{ij},\tilde{k}_{ij}$ and $\tilde{\chi}_{ij}$ illustrate modified properties for plane stress state

$$\tilde{c}_{11}=c_{11}-\frac{c_{13}^2}{c_{33}},\ \tilde{c}_{12}=c_{12}-\frac{c_{13}^2}{c_{33}},\ \tilde{c}_{66}=c_{66},\ \ \tilde{e}_{15}=e_{15},\ \ \tilde{e}_{31}=e_{31}-\frac{c_{13}e_{33}}{c_{33}},$$
$$\tilde{q}_{15}=q_{15},\ \tilde{q}_{31}=q_{31}-\frac{c_{13}q_{33}}{c_{33}},\ \ \tilde{d}_{11}=\tilde{d}_{11},\ \ \tilde{d}_{33}=\tilde{d}_{33}+\frac{q_{33}e_{33}}{c_{33}},\qquad (25)$$
$$\tilde{k}_{11}=k_{11},\ \ \tilde{k}_{33}=k_{33}+\frac{e_{33}^2}{c_{33}},\ \ \tilde{\chi}_{11}=\chi_{11},\ \ \tilde{\chi}_{33}=\chi_{33}+\frac{q_{33}^2}{c_{33}}$$

Integrating the constitutive equations represented in Eqs. (19)-(24) according to the thickness, the below expressions can be derived for a nano-size piezo-magnetic beam

$$(1-(ea)^2\nabla^2)N_x=A_{11}(\frac{\partial u}{\partial x}+\frac{1}{2}(\frac{\partial w}{\partial x})^2)-B_{11}\frac{\partial^2 w_b}{\partial x^2}-B_{11}^s\frac{\partial^2 w_s}{\partial x^2}\qquad (26)$$
$$+A_{31}^e\phi+A_{31}^m\gamma-N_x^E-N_x^H$$

$$(1-(ea)^2\nabla^2)M_x^b=B_{11}(\frac{\partial u}{\partial x}+\frac{1}{2}(\frac{\partial w}{\partial x})^2)-D_{11}\frac{\partial^2 w_b}{\partial x^2}-D_{11}^s\frac{\partial^2 w_s}{\partial x^2}\qquad (27)$$
$$+E_{31}^e\phi+E_{31}^m\gamma$$

$$(1-(ea)^2\nabla^2)M_x^s=B_{11}^s(\frac{\partial u}{\partial x}+\frac{1}{2}(\frac{\partial w}{\partial x})^2)-D_{11}^s\frac{\partial^2 w_b}{\partial x^2}-H_{11}^s\frac{\partial^2 w_s}{\partial x^2}\qquad (28)$$
$$+F_{31}^e\phi+F_{31}^m\gamma$$

$$\int_{-h/2}^{h/2}(1-(ea)^2\nabla^2)D_x\cos(\beta z)dz=E_{15}^e\frac{\partial w_s}{\partial x}+F_{11}^e\frac{\partial\phi}{\partial x}+F_{11}^m\frac{\partial\gamma}{\partial x}\qquad (29)$$

$$(1-(ea)^2\nabla^2)\int_{-h/2}^{h/2}D_z\,\beta\sin(\beta z)dz=A_{31}^e(\frac{\partial u}{\partial x}+\frac{1}{2}(\frac{\partial w}{\partial x})^2)-E_{31}^e\frac{\partial^2 w_b}{\partial x^2}-F_{31}^e\frac{\partial^2 w_s}{\partial x^2}\qquad (30)$$
$$-F_{33}^e\phi-F_{33}^m\gamma$$

$$\int_{-h/2}^{h/2}(1-(ea)^2\nabla^2)B_x\cos(\beta z)dz=E_{15}^m\frac{\partial w_s}{\partial x}+F_{11}^m\frac{\partial\phi}{\partial x}+X_{11}^m\frac{\partial\gamma}{\partial x}\qquad (31)$$

$$\int_{-h/2}^{h/2}(1-(ea)^2\nabla^2)B_z\,\beta\sin(\beta z)dz=A_{31}^m(\frac{\partial u}{\partial x}+\frac{1}{2}(\frac{\partial w}{\partial x})^2)-E_{31}^m\frac{\partial^2 w_b}{\partial x^2}-F_{31}^m\frac{\partial^2 w_s}{\partial x^2}\qquad (32)$$
$$-F_{33}^m\phi-X_{33}^m\gamma$$

$$(1-(ea)^2\nabla^2)Q_{xz}=A_{55}^s\frac{\partial w_s}{\partial x}-A_{15}^e\frac{\partial\phi}{\partial x}-A_{15}^m\frac{\partial\gamma}{\partial x}\qquad (33)$$

So that

$$\{A_{11},B_{11},B_{11}^s,D_{11},D_{11}^s,H_{11}^s\}=\int_{-h/2}^{h/2}\tilde{c}_{11}(1,z,\square,z^2,z\square,\square^2)dz\qquad (34)$$

$$\{A_{31}^e,E_{31}^e,F_{31}^e\}=\int_{-h/2}^{h/2}\tilde{e}_{31}\beta\sin(\beta z)\{1,z,\square\}dz\qquad (35)$$

$$\{A_{31}^m,E_{31}^m,F_{31}^m\}=\int_{-h/2}^{h/2}\tilde{q}_{31}\beta\sin(\beta z)\{1,z,\square\}dz\qquad (36)$$

$$\{F_{11}^e,F_{33}^e\}=\int_{-h/2}^{h/2}\{\tilde{k}_{11}\cos^2(\beta z),\tilde{k}_{33}\beta^2\sin^2(\beta z)\}dz\qquad (37)$$

$$\{F_{11}^m,F_{33}^m\}=\int_{-h/2}^{h/2}\{\tilde{d}_{11}\cos^2(\beta z),\tilde{d}_{33}\beta^2\sin^2(\beta z)\}dz\qquad (38)$$

$$\{X_{11}^m,X_{33}^m\}=\int_{-h/2}^{h/2}\{\tilde{\chi}_{11}\cos^2(\beta z),\tilde{\chi}_{33}\beta^2\sin^2(\beta z)\}dz\qquad (39)$$

$$A_{55}^s=\int_{-h/2}^{h/2}\tilde{c}_{66}r^2dz\qquad (40)$$

$$\{A_{15}^e,E_{15}^e\}=\int_{-h/2}^{h/2}\tilde{e}_{15}\cos(\beta z)\{1,r\}dz\qquad (41)$$

$$\{A_{15}^m,E_{15}^m\}=\int_{-h/2}^{h/2}\tilde{q}_{15}\cos(\beta z)\{1,r\}dz\qquad (42)$$

Applied electro-magnetic force and moments provided in Eq. (26) can be defined as follows

$$N_x^E=-\int_{-h/2}^{h/2}\tilde{e}_{31}\frac{2V_E}{h}dz,\ \ N_x^H=-\int_{-h/2}^{h/2}\tilde{q}_{31}\frac{2\Omega}{h}dz\qquad (43)$$

Five governing equations presented as Eqs. (8)-(12) can be represented in terms of displacements by placing Eqs. (26)-(33) in them as

$$A_{11}(\frac{\partial^2 u}{\partial x^2}+\frac{\partial w}{\partial x}\frac{\partial^2 w}{\partial x^2})-B_{11}\frac{\partial^3 w_b}{\partial x^3}-B_{11}^s\frac{\partial^3 w_s}{\partial x^3}+A_{31}^e\frac{\partial\phi}{\partial x}+A_{31}^m\frac{\partial\gamma}{\partial x}=0\qquad (44)$$

$$-D_{11}\frac{\partial^4 w_b}{\partial x^4}-D_{11}^s\frac{\partial^4 w_s}{\partial x^4}+E_{31}^e(\frac{\partial^2\phi}{\partial x^2})+E_{31}^m(\frac{\partial^2\gamma}{\partial x^2})-A_{15}^e(\frac{\partial^2\phi}{\partial x^2})-A_{15}^m(\frac{\partial^2\gamma}{\partial x^2})$$
$$+(1-(ea)^2\nabla^2)(f(t)-I_0\frac{\partial^2(w_b+w_s)}{\partial t^2}-I_1(\frac{\partial^3 u}{\partial x\partial t^2})+I_2(\frac{\partial^4 w_b}{\partial x^2\partial t^2})+J_2(\frac{\partial^4 w_s}{\partial x^2\partial t^2})\qquad (45)$$
$$+\left(A_{11}(\frac{\partial u}{\partial x}+\frac{1}{2}(\frac{\partial w}{\partial x})^2)-B_{11}\frac{\partial^2 w_b}{\partial x^2}-B_{11}^s\frac{\partial^2 w_s}{\partial x^2}+A_{31}^e\phi+A_{31}^m\gamma-N_x^E-N_x^H\right)$$
$$-k_L w+k_P\frac{\partial^2 w}{\partial x^2}-k_{NL}w^3)[\frac{\partial^2 w}{\partial x^2}]=0$$

$$-D_{11}^s\frac{\partial^4 w_b}{\partial x^4}-H_{11}^s\frac{\partial^4 w_s}{\partial x^4}+A_{55}^s\frac{\partial^2 w_s}{\partial x^2}+F_{31}^e(\frac{\partial^2\phi}{\partial x^2})+F_{31}^m(\frac{\partial^2\gamma}{\partial x^2})-A_{15}^e(\frac{\partial^2\phi}{\partial x^2})-A_{15}^m(\frac{\partial^2\gamma}{\partial x^2})$$
$$+(1-(ea)^2\nabla^2)(f(t)-I_0\frac{\partial^2(w_b+w_s)}{\partial t^2}-J_1(\frac{\partial^3 u}{\partial x\partial t^2})+J_2(\frac{\partial^4 w_b}{\partial x^2\partial t^2})+K_2(\frac{\partial^4 w_s}{\partial x^2\partial t^2})\qquad (46)$$
$$+\left(A_{11}(\frac{\partial u}{\partial x}+\frac{1}{2}(\frac{\partial w}{\partial x})^2)-B_{11}\frac{\partial^2 w_b}{\partial x^2}-B_{11}^s\frac{\partial^2 w_s}{\partial x^2}+A_{31}^e\phi+A_{31}^m\gamma-N_x^E-N_x^H\right)$$
$$-k_L w+k_P\frac{\partial^2 w}{\partial x^2}-k_{NL}w^3)[\frac{\partial^2 w}{\partial x^2}]=0$$

$$A_{31}^e(\frac{\partial u}{\partial x}+\frac{1}{2}(\frac{\partial w}{\partial x})^2)-E_{31}^e(\frac{\partial^2 w}{\partial x^2})-(F_{31}^e-E_{15}^e)(\frac{\partial^2 w_s}{\partial x^2})+F_{11}^e(\frac{\partial^2\phi}{\partial x^2})+F_{11}^m(\frac{\partial^2\gamma}{\partial x^2})\qquad (47)$$
$$-F_{33}^e\phi-F_{33}^m\gamma=0$$

$$A_{31}^m(\frac{\partial u}{\partial x}+\frac{1}{2}(\frac{\partial w}{\partial x})^2)-E_{31}^m(\frac{\partial^2 w}{\partial x^2})-(F_{31}^m-E_{15}^m)(\frac{\partial^2 w_s}{\partial x^2})+F_{11}^m(\frac{\partial^2\phi}{\partial x^2})+X_{11}^m(\frac{\partial^2\gamma}{\partial x^2})\qquad (48)$$
$$-F_{33}^m\phi-X_{33}^m\gamma=0$$

It is also possible to reduce the number of above governing equations to three equation by deriving $\partial u/\partial x$ from Eq. (44) and then substituting it in Eqs. (45)-(48). Thus, knowing this fact that axial inertia has negligible impact on transversal vibrations, Eq. (44) becomes

$$A_{11}(\frac{\partial u}{\partial x}+\frac{1}{2}(\frac{\partial w}{\partial x})^2)-B_{11}\frac{\partial^2 w_b}{\partial x^2}-B_{11}^s\frac{\partial^2 w_s}{\partial x^2}\qquad (49)$$
$$+A_{31}^e\phi+A_{31}^m\gamma-N_x^E-N_x^H=C_1$$

Then

$$\frac{\partial u}{\partial x}=-\frac{1}{2}(\frac{\partial w}{\partial x})^2-\frac{A_{31}^e}{A_{11}}\phi-\frac{A_{31}^m}{A_{11}}\gamma+\frac{B_{11}}{A_{11}}\frac{\partial^2 w_b}{\partial x^2}+\frac{B_{11}^s}{A_{11}}\frac{\partial^2 w_s}{\partial x^2}\qquad (50)$$
$$+\frac{N_x^E}{A_{11}}+\frac{N_x^H}{A_{11}}+\frac{C_1}{A_{11}}$$

Next, integrating Eq. (50) yields

$$u=-\frac{1}{2}\int_0^x(\frac{\partial w}{\partial x})^2dx-\frac{A_{31}^e}{A_{11}}\int_0^x\phi dx-\frac{A_{31}^m}{A_{11}}\int_0^x\gamma dx+\frac{B_{11}}{A_{11}}\frac{\partial w_b}{\partial x}+\frac{B_{11}^s}{A_{11}}\frac{\partial w_s}{\partial x}$$
$$+\frac{N_x^E}{A_{11}}\int_0^x dx+\frac{N_x^H}{A_{11}}\int_0^x dx+\frac{C_1}{A_{11}}x+C_2 \tag{51}$$

Then, by satisfying edge conditions $u(0)=0$, $u(L)=0$, one can derive

$$C_2=-(\frac{B_{11}}{A_{11}}\frac{\partial w_b}{\partial x}+\frac{B_{11}^s}{A_{11}}\frac{\partial w_s}{\partial x})_{x=0}$$
$$C_1=\frac{A_{11}}{2L}\int_0^L(\frac{\partial w}{\partial x})^2dx+\frac{A_{31}^e}{L}\int_0^L\phi dx+\frac{A_{31}^m}{L}\int_0^L\gamma dx \tag{52}$$
$$-(\frac{B_{11}}{L}\frac{\partial w_b}{\partial x}+\frac{B_{11}^s}{L}\frac{\partial w_s}{\partial x})_{x=L}-(N_x^E+N_x^H)$$

As the next step, finded constant must be situated in Eq. (50).

4. Solution method

In this part, by employing Galerkin's approach, the governing equations of motion for free/forced vibrations of simply-supported MEE nano-size beam have been solved. The displacement functions are provided as product of non-unknowns coefficients and known trigonometric functions to assure the boundary conditions at $x=0$ and $x=L$ as (Barati 2017)

$$w_b=\sum_{p=1}^{\infty}W_{bp}(t)X_p(x) \tag{53}$$

$$w_s=\sum_{p=1}^{\infty}W_{sp}(t)X_p(x) \tag{54}$$

$$\phi=\sum_{p=1}^{\infty}\Phi_p(t)X_p(x) \tag{55}$$

$$\gamma=\sum_{p=1}^{\infty}\Upsilon_p(t)X_p(x) \tag{56}$$

where (W_{bp} , W_{sp}, Φ_p, γ_p) display the field largest values and the function $X_p=\sin(p\pi x/L)$ displays the shape function of simply supported beam ($w=\frac{\partial^2 w}{\partial x^2}=\gamma=\phi=0$). Placing Eqs. (53)-(56) in governing equations yields below equations

$$K_{1,1}^S W_{bp}+K_{2,1}^S W_{sp}+G_1W_p^3+Q_1W_p^2+M_1\ddot{W}_p+K_1^E\Phi_p+K_1^H\Upsilon_p=F\cos(\omega t)$$
$$K_{1,2}^S W_{bp}+K_{2,2}^S W_{sp}+G_2W_p^3+Q_2W_p^2+M_2\ddot{W}_p+K_2^E\Phi_p+K_2^H\Upsilon_p=F\cos(\omega t)$$
$$K_{1,3}^S W_{bp}+K_{2,3}^S W_{sp}+G_3W_p^2+K_3^E\Phi_p+K_3^H\Upsilon_p=0 \tag{57}$$
$$K_{1,4}^S W_{bp}+K_{2,4}^S W_{sp}+G_4W_p^2+K_4^E\Phi_p+K_4^H\Upsilon_p=0$$

in which K^S are the components of stiffness matrix and G_i are nonlinear stiffness. The above equations are simultaneously solved in order to obtain nonlinear vibration frequencies. It should be supposed that the approximate solution has below definition

$$W_p(t)=\tilde{W}\cos(\omega t) \tag{58}$$

Also, dimensionless quantities are selected as

$$K_L=\mathrm{k}_L\frac{\mathrm{L}^4}{D_{11}},\ K_p=\mathrm{k}_p\frac{\mathrm{L}^2}{D_{11}},\ K_{NL}=\mathrm{k}_{NL}\frac{\mathrm{L}^4}{A_{11}}$$
$$\tilde{\omega}=\omega L^2\sqrt{\frac{\rho A}{\tilde{c}_{11}I}},\mu=\frac{ea}{L},\tilde{F}=F\frac{L^2}{A_{11}h} \tag{59}$$

5. Numerical results and discussions

Throughout the present section, several graphical examples have been presented and also obtained results have been discussed to survey the correctness of the presented theory in evaluating the free vibrational properties of multi-phase MEE nano-size beams. Obtained results have been provided from the geometrically perfect assumption for the nanobeam. The magnitude of length for nano-scale beam has been chosen to be L=10 nm. For corroborating the reliability of the presented approach, the obtained findings have been compared with the work of Li *et al.* (2018) for the non-linear vibration frequencies of imperfect nanobeam based on a variety of maximum vibration amplitude ($\tilde{W}$) presented in Table 2. One can observe that the results are in accordance with those provided by Li *et al*. (2018) which demonstrate the efficient of the present model.

Influences of piezoelectric volume on forced vibrational curves of the nanobeam is shown in Fig. 2 considering $\tilde{F}$=0.01. The volume of piezoelectric ingredient has been selected to be V_f=0 %, 40% and 80%. From the figure, it may be understand that enhancing the volume of piezoelectric ingredient yields lower shift frequencies. This is associated with the decrement in the elastic stiffness of nano-scale beams by increasing in piezoelectric portion. Afterwards, the elastic modulus of composites decreases by increasing in piezoelectric ingredient as presented in Table 1. Also, as the magnitude of electric voltage is lower, the curves are closer to each other. Accordingly, a MEE nano-scale beam with higher percentages of piezoelectric ingredient is more susceptible to the induced electrical fields.

Fig. 3 provides a comparison among non-linear frequencies based upon classical and improved (refined) shear deformation beam types of MEE nano-sized beam. The presented graph has been illustrated according to the hypothesis that the aspect ratio is L/h=10. This figure highlights that non-linear vibrational curves tend to higher frequencies when the magnitudes of non-dimension deflection growths. Such observation is associated with stiffening influences of non-linear geometrical factors. Moreover, one may understand that improved beam theory grants smaller non-linear vibrational frequencies than

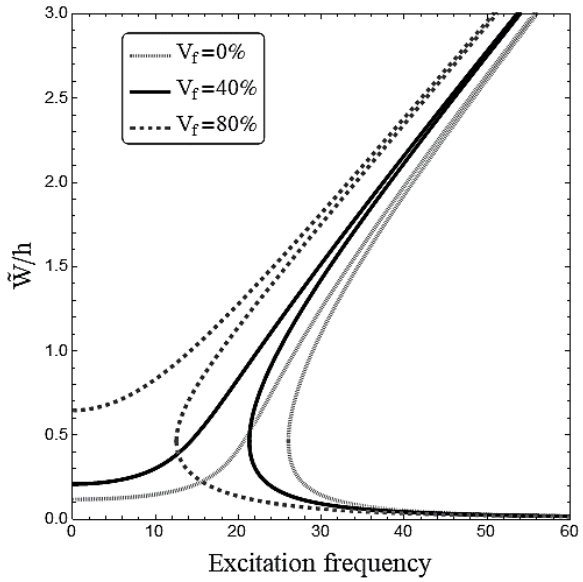

Fig. 2 Impact of piezoelectric percentage and electric voltage on vibration frequency curves of the nanobeam (V_E=0.02V, μ=0.2, Ω=0, K_L=100, K_P=20, K_{NL}=0)

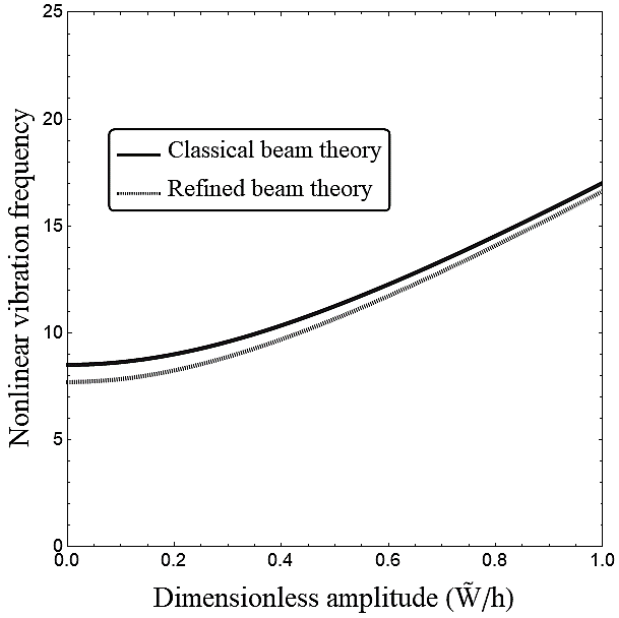

Fig. 3 Comparison among the frequencies based upon classical and refined beam types (V_f=20 %, μ=0.2, V_E=0, L/h=10)

classical theory because of the insertion of shear deformation impact. Hence, the improved theory is more reliable for a thick intelligent piezoelectric-magnetic beam.

Fig. 4 indicates the efficacy of the small scales on the non-linear vibrational frequency of two-phase MEE nano-size beam versus normalized vibrational amplitudes ($\widetilde{W}/h$). It may be seen that as the dimensionless nonlocal parameter (μ) enhances, the normalized frequency declines. Afterwards, it may be deduced that the classical elastic (i.e., the local) theory, which does not incorporate the small size impacts, will provide the higher approximations for the normalized vibrational frequency. However, the nonlocal continuum mechanics will give more precise and dependable results.

Changes of non-linear vibration frequency versus normalized amplitude in various electric voltage (V_E) and magnetic field intensity (Ω) are respectively presented in Figs. 5 and 6. One can observe that the non-linear shift frequency reduces via changing of applied field from negative to positive voltages. As seen, if magnetic field intensity is increased from negative to positive, non-linear vibration frequency is increased. The reason of this behavior is that MEE material has the ability to absorb magnetism and keep it and by rising magnetic field

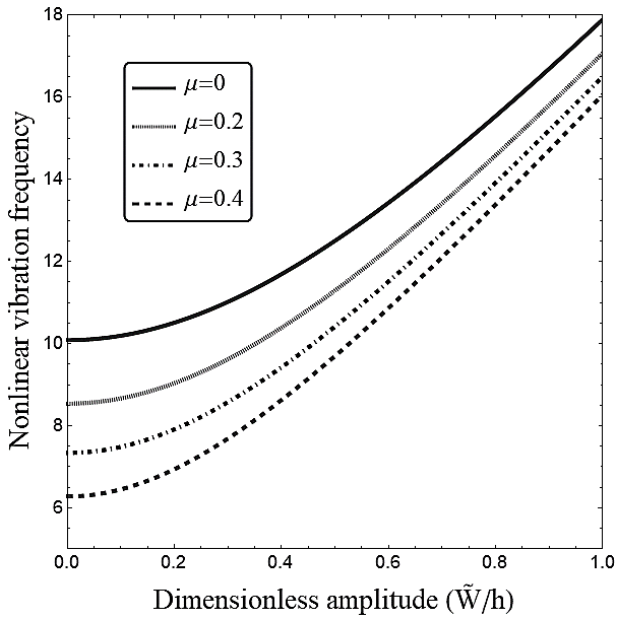

Fig. 4 Impacts of nonlocal factors on the variations of non-linear vibrational frequencies (V_f=20 %, V_E=0, Ω=0)

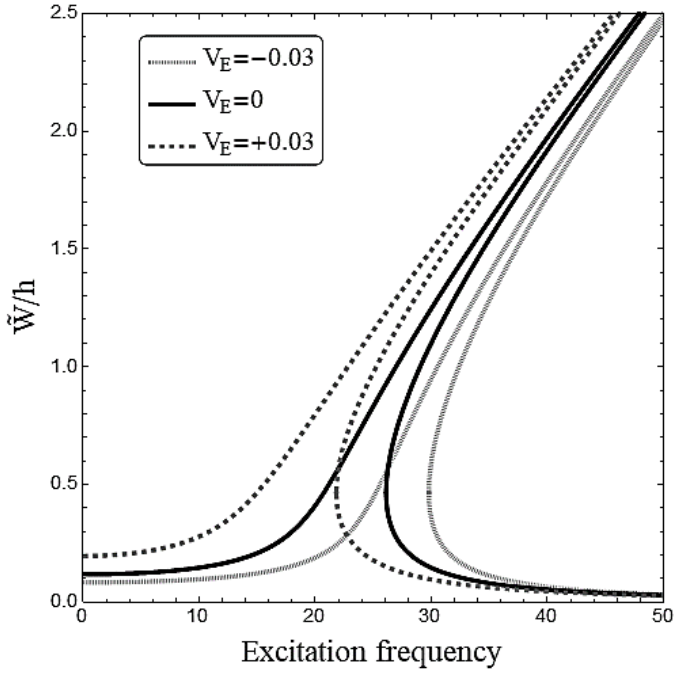

Fig. 5 Effect of applied voltage on vibration frequency curves of the nanobeam (V_f=20 %, μ=0.2, K_L=100, K_P=20, Ω=0)

Table 2 validating the non-linear vibrational frequency for a nanobeam

$\widetilde{W}$=0.2	Li *et al.* (2018)	9.9065
	present	9.9066
$\widetilde{W}$=0.4	Li *et al.* (2018)	10.0166
	present	10.0167

intensity, this ability shows own more. Such materials are capable to convert force of magnetic potential to mechanical force. Thus, via the growth of field intensity, non-linear vibration frequency enlarges because magnetic field creates tensile forces in nanobeam.

Non-dimension deflection of MEE nano-scale beam against non-dimension excitation frequency has been displayed in Figs. 7 and 8 based on diverse substrate coefficients (K_L, K_P, K_{NL}). The amplitude of exerted force is chosen as $\tilde{F} = 0.01$ and the piezoelectric ingredient volume is chosen as V_f=20 %. One may observe that growth

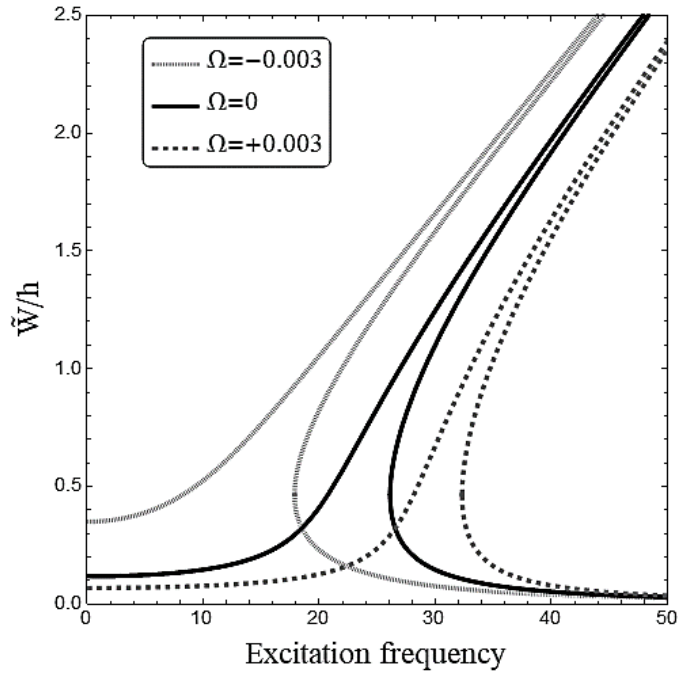

Fig. 6 Effect of magnetic field intensity on vibration frequency curves of the nanobeam (V_f=20 %, μ=0.2, V_E=0, K_L=100, K_P=20, K_{NL}=0)

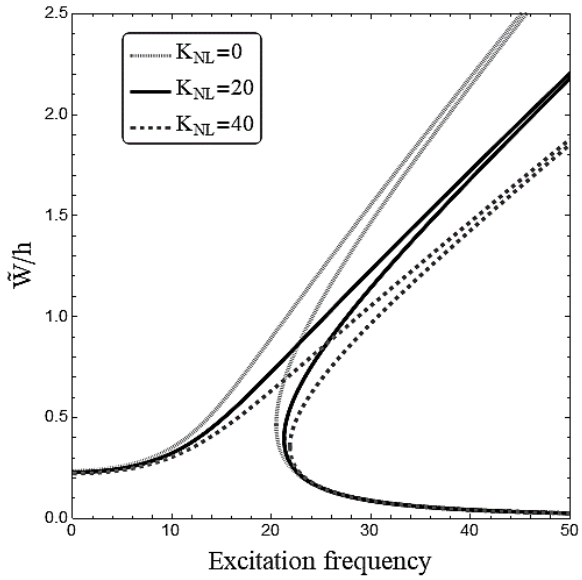

Fig. 7 Effect of elastic foundation parameters on vibration frequency curves of the nanobeam (V_f=20 %, μ=0.2, V_E=0, Ω=0, K_L=100, K_P=0)

of linear (K_L) and shear (K_P) substrate coefficients makes the MEE nano-size beam more rigid leading to greater natural frequencies. As regards, nonlinear substrate coefficient has no influence on the measure of natural frequencies. However, enlarging the values of K_{NL} yields more tendency of frequency-deflection curves to the right. This means that the hardening influences of geometrical nonlinearity become more announced with increase of K_{NL}.

6. Conclusions

The presented research examined nonlocal non-linear free/forced vibrations of two-phase MEE nanobeams by presenting an analytical trend. The nanobeam was assumed to be rested on elastic foundation with a three parameters including linear, shear and nonlinear. It was seen that as the dimensionless nonlocal parameter increases, the normalized frequency decreases. Thus, it can be deduced that the classical elastic (i.e., the local) model, which does not

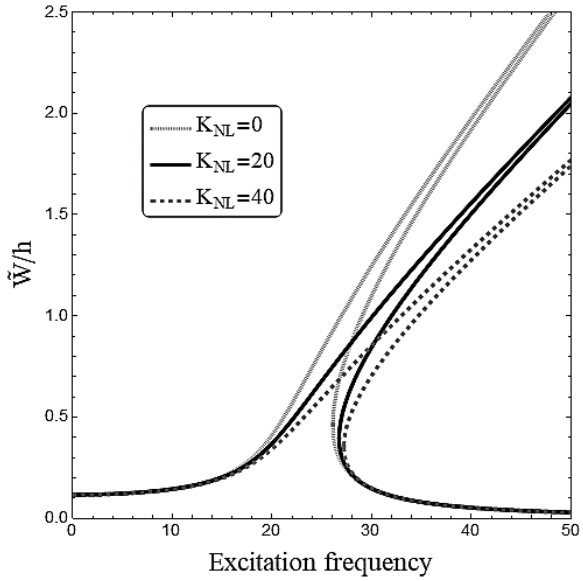

Fig. 8 Effect of elastic foundation parameters on vibration frequency curves of the nanobeam (V_f=20 %, μ=0.2, V_E=0, Ω=0, K_L=100, K_P=20)

consider the small-scale impacts, will give higher approximations for the non-dimension vibrational frequency. However, impact of non-linear foundation parameter on vibration frequency curves has an increasing trend with increasing in vibration amplitude. Also, magnetic field effect on vibration characteristics of MEE nanobeams relies on the value of piezoelectric volume. But, the rate of frequency increment versus magnetic field intensity becomes lower by increase of piezoelectric volume.

Acknowledgements

The authors would like to thank Mustansiriyah university (www.uomustansiriyah.edu.iq) Baghdad-Iraq, for their support in the present work.

References

Abdelaziz, H.H., Meziane, M.A.A., Bousahla, A.A., Tounsi, A., Mahmoud, S.R. and Alwabli, A.S. (2017), "An efficient hyperbolic shear deformation theory for bending, buckling and free vibration of FGM sandwich plates with various boundary conditions", *Steel Compos. Struct.*, **25**(6), 693-704. https://doi.org/10.12989/scs.2017.25.6.693.

Ahmed, R.A., Fenjan, R.M. and Faleh, N.M. (2019), "Analyzing post-buckling behavior of continuously graded FG nanobeams with geometrical imperfections", *Geomech. Eng.*, **17**(2), 175-180. https://doi.org/10.12989/gae.2019.17.2.175.

Al-Maliki, A.F., Faleh, N.M. and Alasadi, A.A. (2019), "Finite element formulation and vibration of nonlocal refined metal foam beams with symmetric and non-symmetric porosities", *Struct. Monit. Maint.*, **6**(2), 147-159. https://doi.org/10.12989/smm.2019.6.2.147.

Annigeri, A.R., Ganesan, N. and Swarnamani, S. (2007), "Free vibration behaviour of multiphase and layered magneto-electro-elastic beam", *J. Sound Vib.*, **299**(1-2), 44-63. https://doi.org/10.1016/j.jsv.2006.06.044.

Atmane, H.A., Tounsi, A., Bernard, F. and Mahmoud, S.R. (2015), "A computational shear displacement model for vibrational analysis of functionally graded beams with porosities", *Steel Compos. Struct.*, **19**(2), 369-384. https://doi.org/10.12989/scs.2015.19.2.369.

Barati, M.R. (2017), "Nonlocal-strain gradient forced vibration analysis of metal foam nanoplates with uniform and graded porosities", *Adv. Nano Res.*, **5**(4), 393. https://doi.org/10.12989/anr.2017.5.4.393.

Bellifa, H., Bakora, A., Tounsi, A., Bousahla, A.A. and Mahmoud, S.R. (2017), "An efficient and simple four variable refined plate theory for buckling analysis of functionally graded plates", *Steel Compos. Struct.*, **25**(3), 257-270. https://doi.org/10.12989/scs.2017.25.3.257.

Besseghier, A., Heireche, H., Bousahla, A. A., Tounsi, A. and Benzair, A. (2015), "Nonlinear vibration properties of a zigzag single-walled carbon nanotube embedded in a polymer matrix," *Advances in nano research*, **3**(1), 029. https://doi.org/10.12989/anr.2015.3.1.029.

Boukhlif, Z., Bouremana, M., Bourada, F., Bousahla, A.A., Bourada, M., Tounsi, A. and Al-Osta, M.A. (2019), "A simple quasi-3D HSDT for the dynamics analysis of FG thick plate on elastic foundation", *Steel Compos. Struct.*, **31**(5), 503-516. https://doi.org/10.12989/scs.2019.31.5.503.

Bounouara, F., Benrahou, K.H., Belkorissat, I. and Tounsi, A. (2016), "A nonlocal zeroth-order shear deformation theory for free vibration of functionally graded nanoscale plates resting on elastic foundation", *Steel Compos. Struct.*, **20**(2), 227-249. https://doi.org/10.12989/scs.2016.20.2.227.

Boutaleb, S., Benrahou, K. H., Bakora, A., Algarni, A., Bousahla, A.A., Tounsi, A. and Mahmoud, S.R. (2019), "Dynamic analysis of nanosize FG rectangular plates based on simple nonlocal quasi 3D HSDT", *Adv. Nano Res.*, **7**(3), 191. https://doi.org/10.12989/anr.2019.7.3.191.

Chaabane, L.A., Bourada, F., Sekkal, M., Zerouati, S., Zaoui, F.Z., Tounsi, A. and Tounsi, A. (2019), "Analytical study of bending and free vibration responses of functionally graded beams resting on elastic foundation", *Struct. Eng. Mech.*, **71**(2), 185-196. https://doi.org/10.12989/sem.2019.71.2.185.

Ebrahimi, F. and Barati, M.R. (2017), "Surface effects on the vibration behavior of flexoelectric nanobeams based on nonlocal elasticity theory", *The European Physical Journal Plus*, **132**(1), 19. https://doi.org/10.1140/epjp/i2017-11320-5.

Eringen, A.C. (1972), "Linear theory of nonlocal elasticity and dispersion of plane waves", *Int. J. Eng. Sci.*, **10**(5), 425-435. https://doi.org/10.1016/0020-7225(72)90050-X.

Fenjan, R.M., Ahmed, R.A., Alasadi, A.A. and Faleh, N.M. (2019), "Nonlocal strain gradient thermal vibration analysis of double-coupled metal foam plate system with uniform and non-uniform porosities", *Coupled Syst Mech*., **8**(3), 247-257. https://doi.org/10.12989/csm.2019.8.3.247.

Fourn, H., Atmane, H.A., Bourada, M., Bousahla, A.A., Tounsi, A. and Mahmoud, S.R. (2018), "A novel four variable refined plate theory for wave propagation in functionally graded material plates", *Steel Compos. Struct.*, **27**(1), 109-122. https://doi.org/10.12989/scs.2018.27.1.109.

Jandaghian, A.A. and Rahmani, O. (2016), "Free vibration analysis of magneto-electro-thermo-elastic nanobeams resting on a Pasternak foundation", *Smart Mater. Struct.*, **25**(3), 035023. https://doi.org/10.1088/0964-1726/25/3/035023.

Karami, B., Janghorban, M. and Tounsi, A. (2017), "Effects of triaxial magnetic field on the anisotropic nanoplates", *Steel Compos. Struct.*, **25**(3), 361-374. https://doi.org/10.12989/scs.2017.25.3.361.

Ke, L.L. and Wang, Y. S. (2014), "Free vibration of size-dependent magneto-electro-elastic nanobeams based on the nonlocal theory", *Physica E: Low-Dimensional Syst. Nanostruct.*, **63**, 52-61. https://doi.org/10.1016/j.physe.2014.05.002.

Kumaravel, A., Ganesan, N. and Sethuraman, R. (2007), "Buckling and vibration analysis of layered and multiphase magneto-electro-elastic beam under thermal environment", *Multidiscipline Model. Mater. Struct.*, **3**(4), 461-476. https://doi.org/10.1163/157361107782106401.

Li, L. and Hu, Y. (2016), "Critical flow velocity of fluid-conveying magneto-electro-elastic pipe resting on an elastic foundation", *Int. J. Mech. Sci.*, **119**, 273-282. https://doi.org/10.1016/j.ijmecsci.2016.10.030.

Li, L., Tang, H. and Hu, Y. (2018), "Size-dependent nonlinear vibration of beam-type porous materials with an initial geometrical curvature", *Compos. Struct.*, **184**, 1177-1188. https://doi.org/10.1016/j.compstruct.2017.10.052.

Mahmoudi, A., Benyoucef, S., Tounsi, A., Benachour, A., Adda Bedia, E.A. and Mahmoud, S.R. (2019), "A refined quasi-3D shear deformation theory for thermo-mechanical behavior of functionally graded sandwich plates on elastic foundations", *J. Sandw. Struct. Mater.*, **21**(6), 1906-1929. https://doi.org/10.1177%2F1099636217727577.

Medani, M., Benahmed, A., Zidour, M., Heireche, H., Tounsi, A., Bousahla, A.A. and Mahmoud, S.R. (2019), "Static and dynamic behavior of (FG-CNT) reinforced porous sandwich plate using energy principle", *Steel Compos. Struct.*, **32**(5), 595-610. https://doi.org/10.12989/scs.2019.32.5.595.

Mirjavadi, S.S., Forsat, M., Nikookar, M., Barati, M.R and Hamouda, A.M.S. (2019), "Nonlinear forced vibrations of sandwich smart nanobeams with two-phase piezo-magnetic face sheets", *The European Physical Journal Plus*, **134**(10), 508. https://doi.org/10.1140/epjp/i2019-12806-8.

Pan, E. and Han, F. (2005), "Exact solution for functionally graded and layered magneto-electro-elastic plates", *Int. J. Eng. Sci.*, **43**(3-4), 321-339. https://doi.org/10.1016/j.ijengsci.2004.09.006.

Saffari, S., Hashemian, M. and Toghraie, D. (2017), "Dynamic stability of functionally graded nanobeam based on nonlocal Timoshenko theory considering surface effects," *Physica B: Condensed Matter*, **520**, 97-105. https://doi.org/10.1016/j.physb.2017.06.029.

Sahu, S.A., Singhal, A. and Chaudhary, S. (2018), "Surface wave propagation in functionally graded piezoelectric material: an analytical solution", *J. Intel. Mat. Syst. Str.*, **29**(3), 423-437. https://doi.org/10.1177%2F1045389X17708047.

Semmah, A., Heireche, H., Bousahla, A.A. and Tounsi, A. (2019), "Thermal buckling analysis of SWBNNT on Winkler foundation by non local FSDT", *Adv. Nano Res.*, **7**(2), 89. https://doi.org/10.12989/anr.2019.7.2.089.

She, G.L., Ren, Y.R., Yuan, F.G. and Xiao, W.S. (2018), "On vibrations of porous nanotubes", *Int. J. Eng. Sci.*, **125**, 23-35. https://doi.org/10.1016/j.ijengsci.2017.12.009.

She, G.L., Yan, K.M., Zhang, Y.L., Liu, H.B. and Ren, Y.R. (2018), "Wave propagation of functionally graded porous nanobeams based on non-local strain gradient theory", *The European Physical Journal Plus*, **133**(9), 368. https://doi.org/10.1140/epjp/i2018-12196-5.

Singhal, A., Sahu, S.A. and Chaudhary, S. (2018), "Liouville-Green approximation: An analytical approach to study the elastic waves vibrations in composite structure of piezo material", *Compos. Struct.*, **184**, 714-727. https://doi.org/10.1016/j.compstruct.2017.10.031.

Soltani, K., Bessaim, A., Houari, M.S.A., Kaci, A., Benguediab, M., Tounsi, A. and Alhodaly, M.S. (2019), "A novel hyperbolic shear deformation theory for the mechanical buckling analysis of advanced composite plates resting on elastic foundations", *Steel Compos. Struct.*, **30**(1), 13-29. https://doi.org/10.12989/scs.2019.30.1.013.

Tlidji, Y., Zidour, M., Draiche, K., Safa, A., Bourada, M., Tounsi, A. and Mahmoud, S.R. (2019), "Vibration analysis of different material distributions of functionally graded microbeam", *Struct. Eng. Mech.*, **69**(6), 637-649. https://doi.org/10.12989/sem.2019.69.6.637.

Uzun, B. and Civalek, Ö. (2019), "Free vibration analysis Silicon nanowires surrounded by elastic matrix by nonlocal finite element method", *Adv. Nano Res.*, **7**(2), 99. https://doi.org/10.12989/anr.2019.7.2.099.

Wu, C.P., Chen, Y.H., Hong, Z.L. and Lin, C.H. (2018), "Nonlinear vibration analysis of an embedded multi-walled carbon nanotube", *Adv. Nano Res.*, **6**(2), 163. https://doi.org/10.12989/anr.2018.6.2.163.

Zarga, D., Tounsi, A., Bousahla, A.A., Bourada, F. and Mahmoud, S.R. (2019), "Thermomechanical bending study for functionally graded sandwich plates using a simple quasi-3D shear deformation theory," *Steel and Composite Structures*, **32**(3), 389-410. https://doi.org/10.12989/scs.2019.32.3.389.

CC